VOL. 13, NO. 19, OCTOBER 2018 ISSN 1819-6608
ARPN Journal of Engineering and Applied Sciences
©2006-2018 Asian Research Publishing Network (ARPN). All rights reserved.
www.arpnjournals.com

STRUCTURAL, ELECTRICAL AND MAGNETIC PROPERTIES OF THE ($Ce_xFe_{0.05}Mg_{0.95-x}O$) NANO COMPOUND SYNTHESIZED VIA SOL-GEL / AUTO COMBUSTION TECHNIQUE

Ahmed H. Abed[1], Tagreed M. Al- Saadi[2] and Ziad T. Khodair[3]
[1]The General Directorate for Education in Diyala, Diyala, Iraq
[2]Department of Physics, College of Education for Pure Science Ibn Al-Haitham, University of Baghdad, Iraq
[3]Department of Physics, College of Science, University of Diyala, Iraq
E-Mail: tagreedmm2000@gmail.com

ABSTRACT

In this work (Ce_x $Fe_{0.05}Mg_{0.95-x}O$) nanoparticles (where x= 0, 0.025, 0.05, 0.075 and 0.10) were prepared by using sol-gel /auto combustion technique. The XRD results showed that all samples are polycrystalline in nature with cubic structure and lattice constant (a) decrease with increasing of Ce content in the sample. The crystallite size found an average size of (14.26 - 25.21 nm) was estimated by using Debye-Scherrer equation. The results of (SEM) showed that the morphology look like irregular aggregated of particles. The analysis of (EDX) confirmed the presence of Mg, Ce, Fe and O ions in the prepared samples. The results revealed that the dielectric loss factor and dielectric constant increase with increasing the content of Ceion, but the conductivity is inverse that behavior also the results showed that the initial magnetic permeability and relative loss factor were affected by change the content of Ce ion.

Keyword: Nano compound, XRD, SEM, dielectric properties, initial permeability.

1. INTRODUCTION

MgO is Multi-use metal oxides has several applications in many fields such as toxic waste remediation [1], catalysis, antimicrobial materials [2], electrochemical biosensor and refractories [3]. The characteristics of Magnesium oxide depend on the preparation method. There are different methods to prepare magnesium oxide nanoparticles; such as combustion, chemical vapour deposition, sol-gel, precipitation, and many other methods [4, 5].

Doped mineral oxide nanoparticles are salutary in a wide diversity of applications such as photo detectors, dilute magnetic semiconductors, optoelectronics [6]. The insulator oxides, Oxide-based semiconductors with lightened magnetic properties and which can show a ferromagnetic with temperature of Curie above the temperature of the room. These insulator oxides and oxide-based dilute magnetic semiconductors display room temperature- ferromagnetic with just a little percent of a relocating- mineral doping like Co, Ni, Fe, Mn, V, or Cr while grown in powder form, induces important modification in its electric and magnetic properties, etc. Several models of room temperature- ferromagnetic have been proposition for these insulators and semiconductors, consists a new exchanged mechanism including donor electrons in an impurity. [7,8]

The aim of this research is studying the effect of Ce ion on some of the structural, dielectric, and magnetic properties of the ($Ce_xFe_{0.05}MgO$) Nanoparticles prepared by auto combustion technique.

2. EXPERIMENTAL METHOD

The nanoparticles Ce_x $Fe_{0.05}$ $Mg_{0.95-x}$ O were prepared in a sol- gel method and included several stages, as shown in Figure-1:

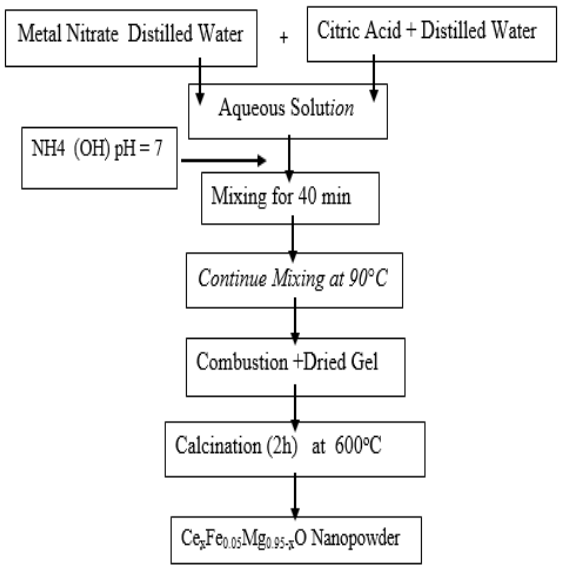

Figure-1. Flow chart of preparation.

The analytical grade of nitrates; $Mg(NO_3)_2$. $6H_2O$, $Fe(NO_3)_3$. $9(H_2O)$,$Ce(NO_3)_3$. $6H_2O$ as a precursor and strict acid $C_6H_8O_7$. H_2O was utilized as a fuel. A certain quantity of strict acid and nitrates was dissolved into distilled water to obtain an aqueous solution. The ratio was used of citric acid: nitrates (0.5:1) molar. The number of pH of solution was adjusted to be 7 using ($NH_4(OH)$). After that, the mixed solution was heated at 90°C under constant stirring .Then, the solution turned from transparent to viscous yellow gel after that this gel became dried, then started to ignition. The combustion was supplementing within a little seconds and loose powder was formed. The precursor was calcined at 600°C for (2 hr) in an atmosphere of air to getting after process

©2006-2018 Asian Research Publishing Network (ARPN). All rights reserved.

is brown color. The samples named as P=pure (MgO), F= ($Fe_{0.05}Mg_{0.95}O$) and D_1, D_2, D_3, D_4= (Ce_x $Fe_{0.05}Mg_{0.95-x}O$) for (x= 0.0, 0.025, 0.05, 0.075 and 0.1) respectively.

3. RESULTS AND DISCUSSIONS

3.1 X-ray powder diffraction

All the peaks that appear in the patterns for all samples were indexed according to (JCPDS 45-0946),so that referred to (fcc) structure [9]. The Miller indices of the peaks of x-ray diffraction are mentioned as appearing in figure (2) and the other peaks referred to presence of iron and cerium. From Figure-2 can observe the intensity of all the XRD peaks decreases with the addition of Fe and Ce-content and this effect is more clear from the plot of the sample in which Ce-content is x = 0.1.

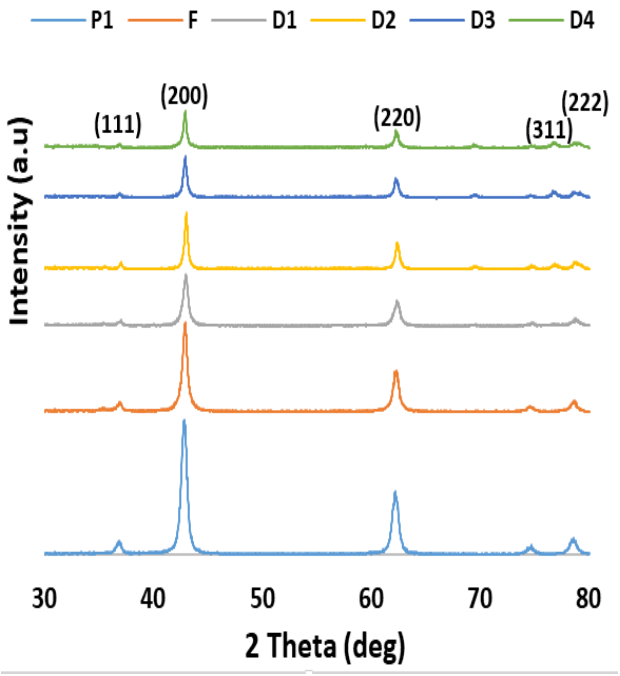

Figure-2. X-ray diffraction patterns of prepared samples.

The average crystallite size (D_{av}) of the nanoparticles was calculated using Debye - Scherrer equation.[10,11]

$D_{av} = K\lambda / \beta \cos\theta$

Where, β: FWHM is the Full Width at Half Maximum), λ: is wavelength, θ: Bragg's angle, and K: is a constant that same to (0.89-0.94). The calculated (D) , (a) and ($\rho_{x\text{-}ray}$) were given in the table (1),from this table can observe that when the content of (Ce^{+4}) increased, the XRD lines shifted towards smallest (2θ) angles showing higher values of lattice constant. The shifting of diffraction lines may be attributed due to the difference in size between the (Ce^{+4}) ions (r= 1.01 Å) and (Mg^{+2}) ions (r= 0.86 Å). On the other hand the values of ($\rho_{x\text{-}ray}$) had same behavior of (a) because the density is depend on the value of lattice constant and the molecular weight of the compound [12],But for the sample F the result is opposite because the radius of ion (Fe^{+2}) (r = 0.75 Å) is smaller than the radius of ion (Ce^{+4}).

Table-1. Variation of Grain size, lattice constant and $\boldsymbol{\rho}_{x\text{-}ray}$ with the Ce concentration.

Sample	D(nm)	a(Å)	$\boldsymbol{\rho}_{x\text{-}ray}$(g/cm^3)	Bulk ($\boldsymbol{\rho}$)(g/cm^3)	Porosity %
P	13.55	4.2036	3.58	2.77	25.24
F	14.42	4.1999	3.67	2.78	25.27
D1	15.36	4.2055	3.81	2.81	26.32
D2	25.21	4.2077	4.05	3.03	34.98
D3	21.59	4.2080	4.31	2.78	29.15
D4	24.3	4.2185	4.35	2.80	31.46

©2006-2018 Asian Research Publishing Network (ARPN). All rights reserved.

3.2 SEM and EDX analysis

The micro structure and morphological studies were carried out using the Scanning Electron Microscope (SEM). The images of samples P, F, and D1 are shown in Figure-3a respectively. From this figures can show irregular aggregated particles that may be due to the high surface energy possessed by small particles or because of difficulties connected with getting higher magnification [13]. The EDX spectra in Figure-3(b) acquired for same samples indicated to presence of Mg has seen at (1.25 KeV), O at (0.525 KeV), Ce at (0.884KeV) and iron at (0.705 KeV).

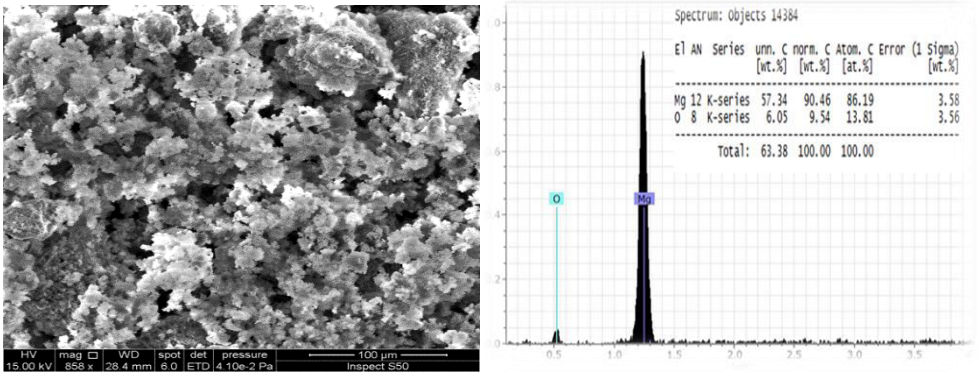

(a)(b)

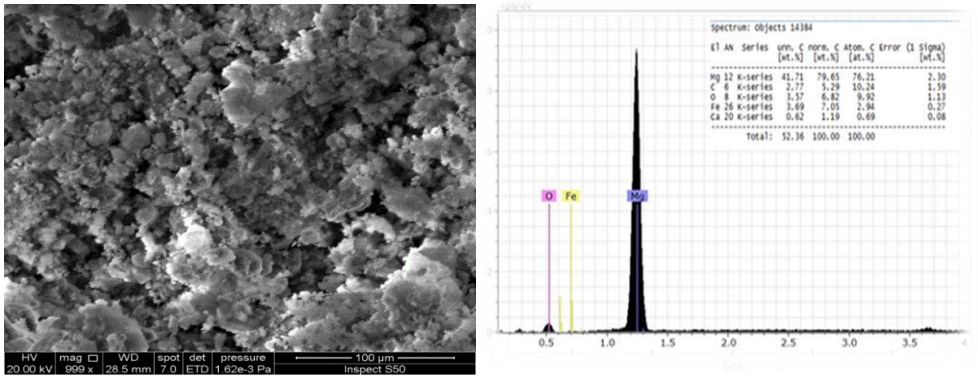

(a) (b)

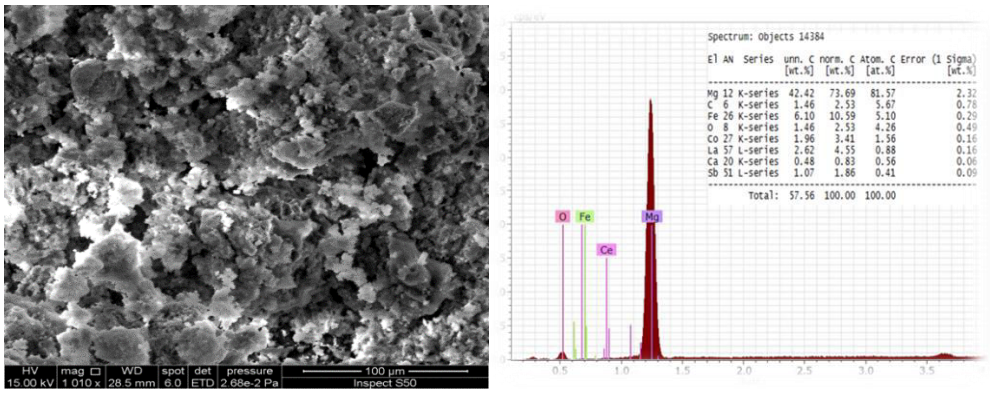

(a) (b)

Figure-3. (a)The SEM (b)The (EDX) of the samples P, F and D_1.

3.3 Dielectric properties

There are three parameters that affected to choose the materials for suitable devices applications, they are; dielectric constant, dielectric Loss and capacitance. The dielectric constant is given by formula:[14]

$$\varepsilon' = C\ d/\varepsilon_o A$$

Where: (d) the thickness of the dielectric sample, (C) the capacitance, (A) the area of the dielectric material and (ε_o) the permittivity of free space. The change in dielectric constant (εr) versus applied frequency for the various samples has taken at room temperature and the results are shown in Figure-4. This may be attributed to the charge lattice defects (the space charge polarization).

©2006-2018 Asian Research Publishing Network (ARPN). All rights reserved.

The bigger values of dielectric constant at few frequencies may be due to the lowest electrostatic binding strength which arises near from the grain boundary surface [15].

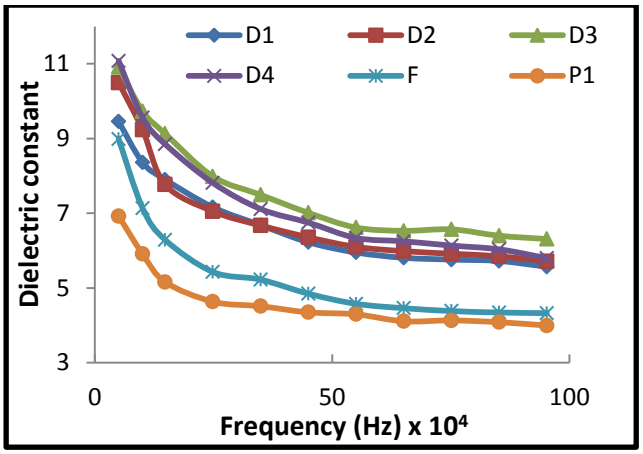

Figure-4. Variation of dielectric constant (ε')with applied frequencyfor the various samples.

The imaginary part of dielectric constant or named dielectric loss factor was calculated by relation [14]:

$\varepsilon'' = \varepsilon' tan\delta$ Where; $\tan\delta$: is the loss tangent.

Figure-5 appeared the change in dielectric loss factor (ε'') with applied frequency for the various samples. The decrease in (ε') with increasing frequency coincides completely with Debye's type of relaxation process [16]. The dielectric loss factor (ε'') noticed to increase with Ce content because cerium oxide is known as low dielectric loss materials. This indicates that the doped samples as a dielectric ceramic; could store extra energy because of the small loss and display good dielectric behavior [17].

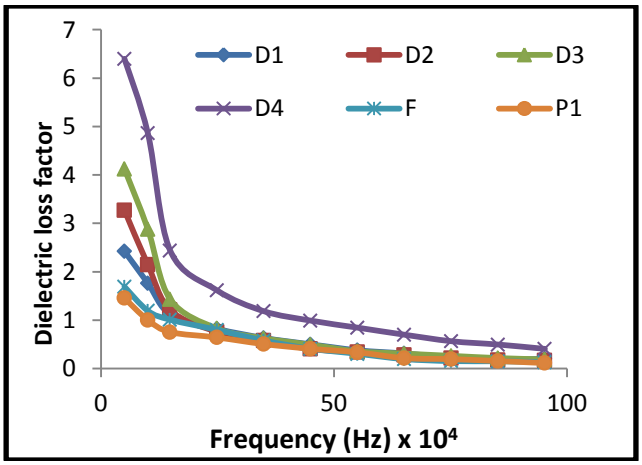

Figure-5. The variation of dielectric loss factor (ε'') versus applied frequency for the various samples.

The electrical conductivity (σ_{ac}):[18] ($\sigma_{ac} = \omega\varepsilon_0\varepsilon''$, ω: the frequency) increases with increase the frequency as shown in Figure-6, this is may be due to the dipole polarization i.e., the twirling of dipoles between two equalized equilibrium locales is involved. It is the automatic alignment of dipoles in one of the equilibrium locales that leads to the nonlinear polarization. The overall comportment of conductivity follows the universe dynamic react, which has broadly been noticed in disordered substance like ionically proceeding glasses and also doped crystalline solids, and is generally thought to be reflected in the mechanism of charge carted behavior of charge carriers [18].

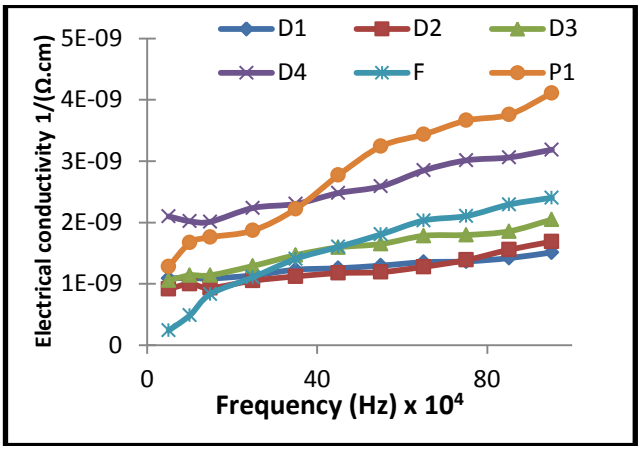

Figure-6. Variation of conductivity($\sigma_{A.c}$)with applied frequency for the various samples.

4. INITIAL MAGNETIC PERMEABILITY AND RELATIVE

4.1 Loss factor

The initial magnetic permeability(μ_i) and relative loss factor (RLF) of all samples were examined by using LCR. The value of (μ_i) was calculated by using the formula [19]:

$$\mu_i = \frac{2\pi L}{2 \times 10^{-7} \times N^2 \times h \times \ln[D_{out}/D_{in}]}$$

Where

L: The induction factor,
N: The number of turns,
D_{out}:The toroid's outer diameter,
D_{in}The toroid's inner diameter, and h height of the toroid.

Figure-7 revealed that (μ_i) decreases as the frequency increases and it is influenced by the Ce ion content. D_2 sample has the highest value of (μ_i), maybe this due to the fact that the grain size would influence straight on the magnetic properties of the materials made from ceramic. Although the move of the domain wall was impeded by pores and grain boundaries but at less grain boundaries with lower pores and results higher initial permeability by easy motion of domain wall [19,20].

©2006-2018 Asian Research Publishing Network (ARPN). All rights reserved.

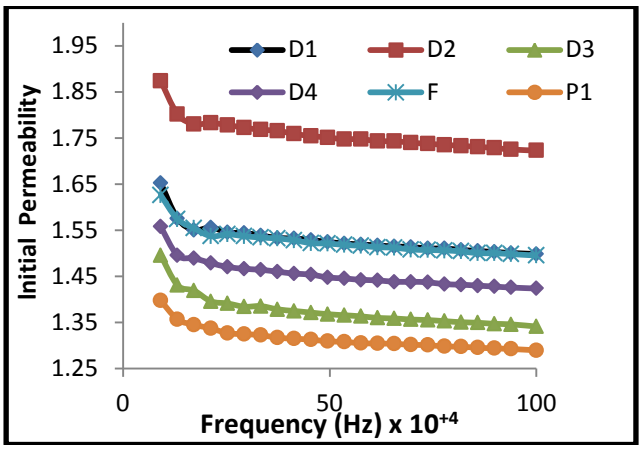

Figure-7. The variation of initial magnetic permeability (μ_i) with applied frequency for the various samples.

Figure-8 appeared the variation of relative loss factor (RLF)with applied frequency for the various samples. All samples have highest relative loss factor at fewer frequencies, that which may be because to highest hysteresis loss altitude from their porosity structures [21].

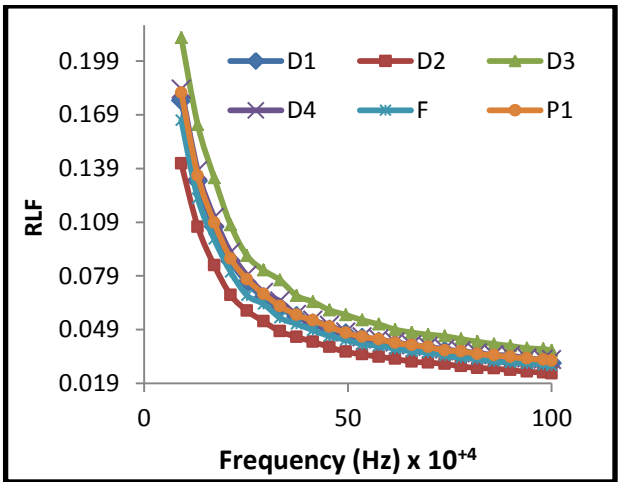

Figure-8. Variation of Relative Loss Factorwith applied frequency for the various samples.

5. CONCLUSIONS

($Ce_xFe_{0.05}Mg_{0.95-x}O$) nanoparticles (where x=0, 0.025, 0.05, 0.075 and 0.10) were synthesized by of sol gel auto-combustion method. XRD results revealed that the prepared samples are polycrystalline in nature with cubic structure. From SEM THE images showed aggregated particles with spherical or semi spherical shapes and (EDX) analysis revealed the presence of Mg, Ce, Fe and O ions in the synthesized samples. The results revealed that the dielectric loss factor and dielectric constant increase with increasing the content of Ceion, but the conductivity is inverse that behavior also the results showed that the initial permeability and relative loss factor were affected by change the content of Ce ion. The $Ce_{0.05}Fe_{0.05}Mg_{0.9}O$ sample showed good crystal structure, fine grain size and good magnetic properties because to high initial magnetic permeability and low loss factor.

REFERENCES

[1] Nirattisai Rakmak, Wisitsree Wiyaratn, Charun Bunyakan, Juntima Chungsiriporn. 2010. Synthesis of Fe/MgO Nano-Crystal Catalysts by Sol-Gel Method for Hydrogen Sulfide Removal. Chemical Engineering. 162(1): 84-90.

[2] Zhang K., An Y., Zhang L. & Dong Q. 2012. Preparation of Controlled Nano-MgO and Investigation of Its Bactericidal Properties. 89(11): 1414-1418.

[3] Braulio M.A.L., Brant P.O.C., Bitterncourt L.R.M. &Pandolfelli V.C. 2009. Microsilica or MgO Grain Size: Which One Mostly affects the in-situ Spinel Refractory Castable Expansion. Ceramics International. 35(8): 3327-3334.

[4] Umar A., Rahman M.M. & Hahn Y. 2009. MgO Polyhedral Nanocages and Nanocrystals Based Glucose Biosensor. Electrochem. Commun. 11(7): 1353-1357.

[5] MohdSufri Mastuli1, Siti Nur Hazlinda Hasbu, Noraziahwati Ibrahim, Mohd Azizi Nawawi. 2014. Effects of Lithium Dopant on Size and Morphology of Magnesium Oxide Nanopowders. Journal of Analytical Sciences. 18(1): 15-20.

[6] Urvashi Sharma P. Jeevanandam. 2015. Synthesis of Zn^{+2} doped MgO Nanoparticles Using Substituted Brucite precursors and studies on their optical properties. Journal of Sol-Gel Science and Technology. 75: 635-648.

[7] S. Azzaza, M. El-Hilo, S. Narayanan, J. Judith Vijaya, N. Mamouni, A. Benyoussef, A. El Kenz, M. Bououdina. 2014. Structural, Optical and Magnetic Characterizations of Mn-doped MgO Nanoparticles. Journal of Materials Chemistry a. 143: 1500 -1507.

[8] Sumalin Phokha, Jutharatana Klinkaewnarong, Sitchai Hunpratub, Kornkanok Boonserm, EkaphanSwatsitang, Santi Maensiri. 2015. Ferromagnetism in Fe-doped MgO Nanoparticles. Journal of Materials Science. 27: 33-39.

[9] Toru H. Okabe, Naoto Sato, Yoshitaka Mitsuda and Sachiko Ono. 2003. Production of Tantalum Powder by Magnesiothermic Reduction of Feed Preform Materials Transactions. Materials Transactions. 44(12): 2646-2653.

©2006-2018 Asian Research Publishing Network (ARPN). All rights reserved.

[10] Farouq I. Hussain and Firas M.Tuamaa. 2016. Synthesis of Nano Compound ($Ba_{1-x}Sr_xTiO_3$) by Sol-Gel Method and Study its Structural Properties. Ibn Al-Haitham J. for Pure & Appl. Sci. 29 (1):417-427.

[11] Ziad T. Khodair, Asaad A. Kamil and Yamamah K. Abdalaah. 2016. Effect of Annealing on Structural and Optical Properties of $Ni_{(1-x)}Mn_xO$ Nanostructures Thin Films. Physica B: Condensed Matter. 503: 55-63.

[12] Khalaf E. Khalil Al- Juboory. 2016. The effect of Cadmium Substitution on the structural and magnetic properties of Nickel Ferrite.Tikrit Journal of Pure Science. 21(2): 155-161.

[13] M. Puchalski, P. Dabrowski, W. Olejniczak, P. Krukowski, P. Kowalczyk, K. Ploanski. 2007.The Study of Silver Nanoparticles by Scanning Electron Microscopy, Energy Dispersive X-Ray Analysis and Scanning Tunnelling Microscopy. Journal of materials science-poland. 2(25): 474-478.

[14] M. Y. Shahid, A. Anwar, F. Malik, M. Asghar, M. F. Warsi,S. Z. Ilyas. 2017. Effect of Sr-Doping On Ferroelectric and Dielectric Properties of Sol-Gel Synthesized Batio3 Thin Films. Digest Journal of Nanomaterials and Biostructures. 12(3): 669-677.

[15] K. Kaviyarasu and Prem Anand Devarajan. 2011. Synthesis and Characterization Studies of Cadmium Doped MgO Nanocrystals for Optoelectronics Application. Journal of Advances in Applied Science Research. 2(6): 131-138.

[16] C. A. F. Vaz, D. Prabhakaran, E. I. Altman, and V. E. Henrich. 2009. 'Experimental study of the interfacial cobalt oxide in Co3O4/α-Al2O3 (0001) epitaxial films. Physical Review B 80:155457, pp. 1-9.

[17] Reza Zamiri, Hossein Abbastabar Ahangar, Ajay Kaushal, Azmi Zakaria, Golnoosh Zamiri, David Tobaldi, and J. M. F. Ferreira. 2015. Dielectrical Properties of CeO_2 Nanoparticles at Different Temperatures. J.PLoS One. 10(4):e0122989.

[18] Pathan Amjad khan Noor khan and Sangshetty Kalayne. 2012. Synthesis, Characterization ac Conductivity of Ni^{+2} Doped in Magnesium Ferrite. Journal of Modern Engineering Research (IJMER). 2: 2303-2306.

[19] Majid Niaz Akhtar, Noorhana Yahya, Patthi Bin Hussain. 2008. Structural and Magnetic characterizations of Nano Structured $Ni_{0.8}Zn_{0.2}Fe_2O_4$ Prepared by Self Combustion Method. Journal of Basic & Applied Sciences. 9(9): 37-40.

[20] S. Zahi, A. R. Daud and M. Hashim. 2007. A comparative study of nickel-zinc ferrites by sol-gel route and solid-state react ion. Materials Chemistry and Physics. 106: 452-456.

[21] P. K.Roy and J. Bera. 2008. Characterized ion of nanocrystalline NiCuZn ferrite powders synthesized by sol-gel auto-combustion method. Journal of Materials Processing Technology. 197: 279-283.